LETTERS

One-to-one coupling of glacial climate variability in Greenland and Antarctica

EPICA Community Members*

Precise knowledge of the phase relationship between climate changes in the two hemispheres is a key for understanding the Earth's climate dynamics. For the last glacial period, ice core studies[1,2] have revealed strong coupling of the largest millennial-scale warm events in Antarctica with the longest Dansgaard–Oeschger events in Greenland[3–5] through the Atlantic meridional overturning circulation[6–8]. It has been unclear, however, whether the shorter Dansgaard–Oeschger events have counterparts in the shorter and less prominent Antarctic temperature variations, and whether these events are linked by the same mechanism. Here we present a glacial climate record derived from an ice core from Dronning Maud Land, Antarctica, which represents South Atlantic climate at a resolution comparable with the Greenland ice core records. After methane synchronization with an ice core from North Greenland[9], the oxygen isotope record from the Dronning Maud Land ice core shows a one-to-one coupling between all Antarctic warm events and Greenland Dansgaard–Oeschger events by the bipolar seesaw[6]. The amplitude of the Antarctic warm events is found to be linearly dependent on the duration of the concurrent stadial in the North, suggesting that they all result from a similar reduction in the meridional overturning circulation.

The glacial climate in the North Atlantic region is characterized by rapid shifts from cold stadial to warmer interstadial conditions[3,4,9]. Greenland temperatures during these Dansgaard–Oeschger (D–O) events rise by 8–16 °C (refs 10, 11) within a few decades followed by a less rapid temperature decline back to stadial conditions. In contrast, glacial climate in the circum-Antarctic region exhibits slower millennial changes with smaller temperature amplitudes of only 1–3 °C (refs 1, 12, 13). After synchronization of Greenland and Antarctic ice core records[1,2] using the global atmospheric change in CH_4 concentrations, a conspicuous phase relationship between the largest Antarctic warmings (A1–A7; ref. 1) and the longest D–O events was observed with the south warming during the stadial conditions in the north, and starting to cool as soon as the D–O warming set in. This bipolar seesaw pattern was explained by changes in the heat and freshwater flux connected to the Atlantic Meridional Overturning Circulation (MOC), where a stronger MOC leads to increased drainage of heat from the Southern Ocean heat reservoir[6,7].

In principle, an interhemispheric climate coupling by the bipolar seesaw should also apply for all the short D–O events. However, to what extent this concept is also able to explain the higher-frequency climate variability in Antarctic ice cores remained unclear (as discussed for example, in ref. 14 and references therein). Here we report

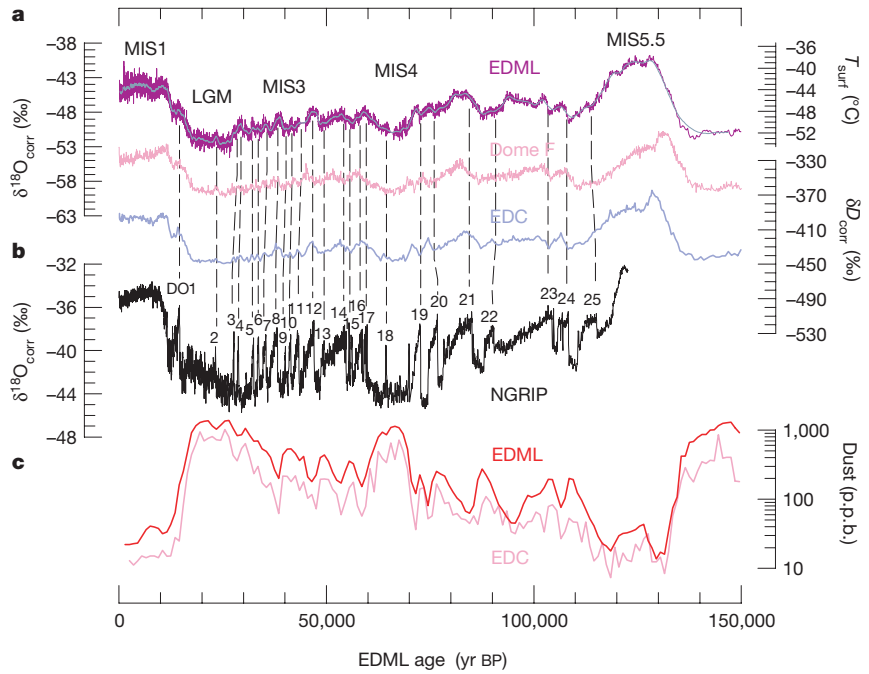

Figure 1 | Antarctic stable isotope records show synchronous millennial variations during the last glacial, whereas rapid variations are encountered in Greenland. a, EDML $\delta^{18}O$ record (purple, 0.5-m resolution; grey, 15-m running mean) after sea level and upstream correction (see Supplementary Information) over the past 150 kyr. The record shows features similar to those of the EDC[12] (blue) and the Dome F[13] (pink) isotope records but with more fine structure during MIS3 and MIS4. We note that EDML and EDC are plotted on the new common EDC3 timescale (see Supplementary Information) while Dome F is plotted on its individual timescale. The temperature axis on the right side indicates approximate surface temperatures at EDML as derived from the spatial $\delta^{18}O$/temperature gradient (see Supplementary Information). **b**, $\delta^{18}O$ record of the NGRIP ice core (grey)[9]. **c**, Mineral dust records of the EDML (red) and EDC[12] (pink) ice cores at 1,000-yr resolution; these dust records were used for synchronization of the cores.

*A full list of authors and their affiliations appears at the end of the paper.

on the climate record over the last glacial cycle from a new ice core drilled within the European Project for Ice Coring in Antarctica (EPICA) in the interior of Dronning Maud Land, hence denoted EDML, at 75° S, 0° E, 2,892 m.a.s.l. (metres above sea level), with a recent accumulation rate of 6.4 cm water equivalent (w.e.) per year[15]. This site was chosen to complement the long EPICA Dome C (EDC, 75° S, 123° E, 3,233 m.a.s.l., 2.5 cm w.e. yr^{-1}) record[12], because EDML is the first deep ice core in the Atlantic sector of the Southern Ocean region[16] and thus located near the southern end of the bipolar seesaw. The snow accumulation at EDML is two to three times higher than at other deep drilling sites on the East Antarctic plateau, so higher-resolution atmosphere and climate records can be obtained for the last glacial period, making the EDML core especially suitable for studying decadal-to-millennial climate variations in Antarctica.

In Fig. 1 the EDML $\delta^{18}O$ record as proxy for local temperature on the ice sheet is shown in 0.5-m resolution (equivalent to 15–30 yr during the marine isotope stage MIS3 and 100–150 yr during MIS5) after correction for upstream and glacial–interglacial ice sheet altitude effects (see Supplementary Information). The overall pattern closely resembles that recorded in most Antarctic ice cores previously covering this time period[12,13,17]. Also, very similar dust profiles (Fig. 1) are encountered at EDML and EDC, related to parallel changes in climate conditions in the Patagonian dust source region common to both cores[18]. Despite the high correlation of the EDML $\delta^{18}O$ and the EDC δD record over the last 150,000 yr ($r^2 = 0.94$ for 250-yr averages) some distinct differences exist. In the penultimate warm period (MIS5.5) the EDML $\delta^{18}O$ record indicates temperatures about 4–5 °C higher than those of the Holocene, in line with other ice cores from the East Antarctic plateau[12,13,17]. However, $\delta^{18}O$ at EDML exhibits persistently higher $\delta^{18}O$ values over the entire duration of MIS5.5 while other ice cores on the East Antarctic plateau show a substantial drop after an initial climate optimum[12,13]. We note that this difference is not due to the altitude corrections applied to the EDML $\delta^{18}O$ record (see Supplementary Information), because a similar temporal evolution during MIS5.5 is also seen in the uncorrected data. Instead, a smaller cooling at EDML in the course of MIS5.5 compared to EDC and Dome Fuji is consistent with marine sediment records from the Atlantic sector of the Southern Ocean revealing persistently warmer summer sea surface temperatures and a reduced winter sea ice cover throughout MIS5.5 (ref. 19). This suggests that there were regional differences in temperature and sea ice evolution during this period for the Atlantic and Indian Ocean sector.

The most outstanding feature of the high-resolution EDML record is the pronounced millennial variability during the glacial. As indicated by the dashed lines in Fig. 1 each of the warming episodes in Antarctica can be related to a corresponding D–O event, but only synchronization of the age scales allows us to assign them unambiguously and to pinpoint the phase relationship between climate changes in Greenland and Antarctica. To do this, the EDML core has been synchronized (see Supplementary Information) to the layer counted NGRIP ice core[20,21] over MIS3, using high-resolution CH_4 profiles over the last 55 kyr from the NGRIP, GRIP and GISP2 ice cores[1,11]. The synchronized $\delta^{18}O$ records are shown in Fig. 2. Also plotted is the CH_4 synchronized $\delta^{18}O$ record from the Byrd ice core[1] and new high-resolution δD data from EDC[22] which closely resemble the temperature variability found at EDML during MIS3 and support an Antarctic-wide interpretation of these fluctuations. The higher glacial snow accumulation at EDML (~3 cm w.e. yr^{-1}) compared to that at EDC, Dome Fuji or Vostok (~1.4 cm w.e. yr^{-1}) implies a CH_4 synchronization two to three times better than at those sites. The synchronization uncertainty for MIS3 ranges from 400 to 800 yr for all events in the EDML record, making the synchronization error for EDML always much smaller than the duration of the events themselves.

This is important, because this allows an unequivocal one-to-one assignment not only of the well-known large warm events in Antarctica (A1, A2 and so on) but of each single isotope maximum indicated in Fig. 2 with a corresponding D–O event in the north. Although the exact timing of the temperature maxima relative to the stadial/interstadial transitions cannot be discerned more precisely than the synchronization error, it is evident that each Antarctic warming starts significantly before the respective D–O event. In addition, a synchronization of the stable water isotope records of the GRIP and EDC ice cores using the ^{10}Be production anomaly around 41,000 yr BP, which constrains the in-phase relationship of the onset of D–O 10 and the respective Antarctic δD maximum to better than 200 yr (ref. 23), supports our CH_4 match. Accordingly, we suggest a new Antarctic Isotope Maximum (AIM) nomenclature in Fig. 2

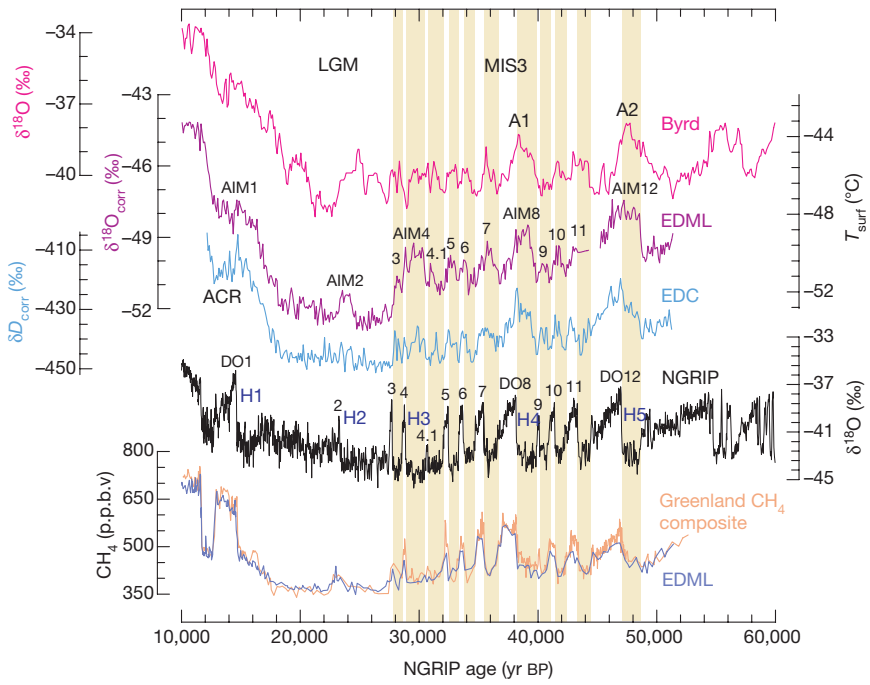

Figure 2 | Methane synchronization of the EDML and the NGRIP records reveals a one-to-one assignment of each Antarctic warming with a corresponding stadial in Greenland. Displayed are 100-yr averages during MIS3 in the EDML, EDC[26] and Byrd[1] ice core for the time interval 10–60 kyr BP in comparison with the NGRIP $\delta^{18}O$ record from Northern Greenland[9]. All records are CH_4 synchronized and given on the new GICC05 age scale for the NGRIP ice core, which has been derived by counting annual layers down to 41 kyr and by a flow model for older ages[9,21]. Yellow bars indicate the Greenland stadial periods that we relate to respective Antarctic temperature increases. The approximate timing of Heinrich layers in North Atlantic sediments is indicated as well[27]. The *y* axis on the right side indicates approximate temperature changes at EDML based on the modern spatial gradient between $\delta^{18}O$ and temperature.

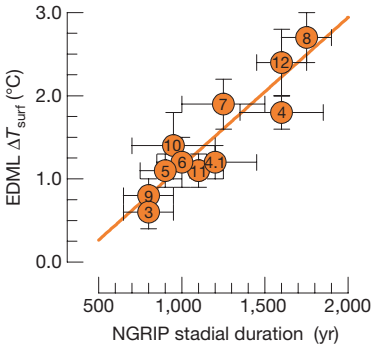

Figure 3 | Amplitudes of Antarctic warmings show a linear relationship ($r^2 = 0.85$) with the duration of the accompanying stadial in Greenland during MIS3. The amplitude was determined from the Antarctic $\delta^{18}O$ maximum to the preceding minimum of each event; the stadial duration is defined by the interval between the midpoint of the stepwise temperature change at the start and end of a stadial on the extended GICC05 age scale[9,21]. Error bars reflect the estimated uncertainty in the definition of the maxima and minima in $\delta^{18}O$ at EDML and in the duration of the concurrent stadial period. Numbers indicate the corresponding AIMs and D–O events.

which reflects the connection of southern warming to reduced oceanic heat transport into the North Atlantic during stadials. The timing and duration of the AIMs relative to D–O events is also indirectly supported by the comparison of changes in deep-water masses linked to Antarctic Bottom Water formation and Atlantic surface water changes, as archived in sediment records offshore of Portugal[24].

Most striking is the varying amplitude of the AIMs, which is linearly dependent on the duration of stadials in the north, as shown in Fig. 3. The only significant deviation from this linear relationship during MIS3 is AIM4, in which the error in the stadial duration estimate is quite large. We conclude that the duration of a reduced MOC—and, hence, the duration of the warming period in the Southern Ocean—determines the amount of heat accumulated in the Southern Ocean heat reservoir, strongly supporting the general applicability of the thermal bipolar seesaw[6] concept within the range of stadial events encountered during MIS3. We note that for longer cessations of the MOC a new equilibrium temperature in the Southern Ocean would be reached and the warming would eventually have to cease. This linear relationship also implies that the Antarctic warming rate—and thus the heat flux from the Southern Ocean to the Atlantic—is similar for all warming events during MIS3. If we assume the same spatial configuration of the overturning cell for cold intervals in MIS3, this would suggest that the strength of the MOC is approximately constant for all stadials, challenging the notion of different overturning rates[25] for stadials in which massive iceberg discharges into the North Atlantic (the so-called Heinrich events in Fig. 2: H1–H5) occurred compared to stadials without Heinrich events. Note however, that the stadials before D–O 8 and D–O 12 in which Heinrich events occurred were the longest and the related Antarctic warmings the largest. This may be due to the longer time needed to mix away the large freshwater anomalies during Heinrich events. There is, however, a less clear relationship for other Heinrich events. Comparison of the millennial climate variability during MIS3 at EDML and EDC shows no significant difference in the amplitude of the isotopic change in the Atlantic and Indian Ocean sectors of the Southern Ocean. This implies a uniform ocean heat reservoir controlling temperature changes at both sites and reflects the rapid mixing of the Southern Ocean by the Antarctic Circumpolar Current.

In the EDML $\delta^{18}O$ record a major warm event (AIM2, connected to D–O 2) is seen during the Last Glacial Maximum, which cannot be clearly identified in the EDC core but is present in the Dome F record (Fig. 1). AIM2 also shows a decrease in high-resolution mineral dust concentrations at EDC, as do all the other AIMs[26]. We therefore conclude that AIM2 is a warm event comparable to the other AIMs in MIS3 but is not sufficiently resolved in the EDC record owing to its lower accumulation. The corresponding D–O 2 event in the North Atlantic is preceded by the longest cold period in the NGRIP record (Fig. 2) and accordingly, a higher temperature amplitude of AIM2 is to be expected if the same bipolar seesaw concept holds as for D–O events during MIS3. However, sea level and temperature conditions were significantly different during the Last Glacial Maximum, potentially affecting the spatial configuration and strength of the overturning cell in the North Atlantic. The fact that AIM2 is only 2,000 yr long suggests that the strength of the MOC was not significantly reduced for the entire cold period in the North, but collapsed only about 1,000 yr before D–O 2, which would be in line with significant iceberg discharge depositing ice-rafted debris in the North Atlantic during H2 (ref. 27).

In summary, a strong interhemispheric coupling of all bipolar climate variations during MIS3 via the MOC is supported by the new high-resolution $\delta^{18}O$ record from EDML indicating that Antarctic warming rates and potentially also overturning rates have been similar for all events in MIS3. The question of what triggers the switch from stadial to interstadial conditions remains. Transitions in the strength of the MOC and its effect on the Atlantic Southern Ocean heat exchange are simulated in response to changes in the North Atlantic freshwater balance[7,8]; however, the origin of such variations in freshwater input are still not ascertained for all individual D–O events. In addition, large iceberg discharge from the Laurentide ice sheet does not systematically coincide with either the onset or the end of stadials[27,28]. Recently, the potential role of a change in Southern Ocean sea-ice cover for reinstalling a stronger MOC has been identified for the onset of the Bølling/Allerød warming[29,30]. The intrinsic feedback of a reduced sea-ice cover in the Southern Ocean during AIMs, followed by a delayed onset of deep-water formation in the North, could potentially explain the interhemispheric climate coupling seen in our records during MIS3.

Received 26 May; accepted 22 September 2006.

1. Blunier, T. & Brook, E. J. Timing of millennial-scale climate change in Antarctica and Greenland during the last glacial period. *Science* **291,** 109–112 (2001).
2. Blunier, T. *et al.* Asynchrony of Antarctic and Greenland climate change during the last glacial period. *Nature* **394,** 739–743 (1998).
3. Johnsen, S. J. *et al.* Irregular glacial interstadials recorded in a new Greenland ice core. *Nature* **359,** 311–313 (1992).
4. Bond, G. *et al.* Correlations between records from North Atlantic sediments and Greenland ice. *Nature* **365,** 143–147 (1993).
5. McManus, J. F., Oppo, D. W. & Cullen, J. L. A 0.5-million-year record of millennial climate variability in the North Atlantic. *Science* **283,** 971–975 (1999).
6. Stocker, T. F. & Johnsen, S. J. A minimum thermodynamic model of the bipolar seesaw. *Paleoceanography* **18,** art. no. 1087 (2003).
7. Knutti, R., Flückiger, J., Stocker, T. F. & Timmermann, A. Strong hemispheric coupling of glacial climate through freshwater discharge and ocean circulation. *Nature* **430,** 851–856 (2004).
8. Ganopolski, A. & Rahmstorf, S. Rapid changes of glacial climate simulated in a coupled climate model. *Nature* **409,** 153–158 (2001).
9. North Greenland Ice Core Project members. High resolution climate record of the northern hemisphere reaching into the last interglacial period. *Nature* **431,** 147–151 (2004).
10. Landais, A. *et al.* Quantification of rapid temperature change during DO event 12 and phasing with methane inferred from air isotopic measurements. *Earth Planet. Sci. Lett.* **225,** 221–232 (2004).
11. Huber, C. *et al.* Isotope calibrated Greenland temperature record over Marine Isotope Stage 3 and its relation to CH_4. *Earth Planet. Sci. Lett.* **245,** 504–519 (2006).
12. EPICA community members. Eight glacial cycles from an Antarctic ice core. *Nature* **429,** 623–628 (2004).
13. Watanabe, O. *et al.* Homogeneous climate variability across East Antarctica over the past three glacial cycles. *Nature* **422,** 509–512 (2003).
14. Roe, G. H. & Steig, E. J. Characterization of millennial-scale climate variability. *J. Clim.* **17,** 1929–1944 (2004).
15. Oerter, H. *et al.* Accumulation rates in Dronning Maud Land, Antarctica, as revealed by dielectric-profiling measurements of shallow firn cores. *Ann. Glaciol.* **30,** 27–34 (2000).
16. Reijmer, C. H., van den Broeke, M. R. & Scheele, M. P. Air parcel trajectories to five deep drilling locations on Antarctica, based on the ERA-15 data set. *J. Clim.* **15,** 1957–1968 (2002).

17. Petit, J. R. *et al.* Climate and atmospheric history of the past 420,000 years from the Vostok ice core, Antarctica. *Nature* **399,** 429–436 (1999).
18. Basile, I. *et al.* Patagonian origin of glacial dust deposited in East Antarctica (Vostok and Dome C) during glacial stages 2, 4 and 6. *Earth Planet. Sci. Lett.* **146,** 573–589 (1997).
19. Bianchi, C. & Gersonde, R. The Southern Ocean surface between Marine Isotope Stage 6 and 5d: Shape and timing of climate changes. *Palaeogeogr. Palaeoclimatol. Palaeoecol.* **187,** 151–177 (2002).
20. Rasmussen, S. O. *et al.* A new Greenland ice core chronology for the last glacial termination. *J. Geophys. Res.* **111,** D06102 (2006).
21. Andersen, K. K. *et al.* The Greenland ice core chronology 2005, 15–42 kyr. Part 1: Constructing the time scale. *Quat. Sci. Rev.* (in the press).
22. Stenni, B. *et al.* A late-glacial high-resolution site and source temperature record derived from the EPICA Dome C isotope records (East Antarctica). *Earth Planet. Sci. Lett.* **217,** 183–195 (2003).
23. Raisbeck, G., Yiou, F. & Jouzel, J. Cosmogenic ^{10}Be as a high resolution correlation tool for climate records. *Geochim. Cosmochim. Acta* **66,** abstr. A623 (2002).
24. Shackleton, N. J., Hall, M. A. & Vincent, E. Phase relationships between millennial-scale events 64,000–24,000 years ago. *Paleoceanography* **15,** 565–569 (2000).
25. Rahmstorf, S. Ocean circulation and climate during the past 120,000 years. *Nature* **419,** 207–214 (2002).
26. Röthlisberger, R. *et al.* Dust and sea-salt variability in central East Antarctica (Dome C) over the last 45 kyrs and its implications for southern high-latitude climate. *Geophys. Res. Lett.* **29,** article no. 1963 (2002).
27. Bond, G. & Lotti, R. Iceberg discharges into the North Atlantic on millennial time scales during the last glaciation. *Science* **267,** 1005–1010 (1995).
28. de Abreu, L., Shackleton, N. J., Joachim Schönfeld, J., Hall, M. & Chapman, M. Millennial-scale oceanic climate variability off the Western Iberian margin during the last two glacial periods. *Mar. Geol.* **196,** 1–20 (2003).
29. Knorr, G. & Lohmann, G. Southern Ocean origin for the resumption of Atlantic thermohaline circulation during deglaciation. *Nature* **424,** 532–536 (2003).
30. Stocker, T. F. & Wright, D. G. Rapid transitions of the ocean's deep circulation induced by changes in surface water fluxes. *Nature* **351,** 729–732 (1991).

Supplementary Information is linked to the online version of the paper at www.nature.com/nature.

Acknowledgements This work is a contribution to the European Project for Ice Coring in Antarctica (EPICA), a joint European Science Foundation/European Commission scientific programme, funded by the EU (EPICA-MIS) and by national contributions from Belgium, Denmark, France, Germany, Italy, the Netherlands, Norway, Sweden, Switzerland and the UK. The main logistic support was provided by IPEV and PNRA (at Dome C) and AWI (at Dronning Maud Land).

Author Information Reprints and permissions information is available at www.nature.com/reprints. The authors declare no competing financial interests. Correspondence and requests for materials should be addressed to H. F. (hufischer@awi-bremerhaven.de).

EPICA Community Members (listed in alphabetical order): C. Barbante[1,2], J.-M. Barnola[3], S. Becagli[4], J. Beer[5], M. Bigler[6,7], C. Boutron[3], T. Blunier[6], E. Castellano[4], O. Cattani[8], J. Chappellaz[3], D. Dahl-Jensen[7], M. Debret[3], B. Delmonte[9], D. Dick[10], S. Falourd[8], S. Faria[10,11], U. Federer[6], H. Fischer[10], J. Freitag[10], A. Frenzel[10], D. Fritzsche[12], F. Fundel[10], P. Gabrielli[2,3], V. Gaspari[1], R. Gersonde[10], W. Graf[13], D. Grigoriev[14], I. Hamann[10], M. Hansson[15], G. Hoffmann[8], M. A. Hutterli[6,16], P. Huybrechts[10,17], E. Isaksson[18], S. Johnsen[7], J. Jouzel[8], M. Kaczmarska[18], T. Karlin[15], P. Kaufmann[6], S. Kipfstuhl[10], M. Kohno[10], F. Lambert[6], Anja Lambrecht[10], Astrid Lambrecht[10], A. Landais[8], G. Lawer[10], M. Leuenberger[6], G. Littot[16], L. Loulergue[3], D. Lüthi[6], V. Maggi[9], F. Marino[9], V. Masson-Delmotte[8], H. Meyer[12], H. Miller[10], R. Mulvaney[16], B. Narcisi[19], J. Oerlemans[20], H. Oerter[10], F. Parrenin[3], J.-R. Petit[3], G. Raisbeck[21], D. Raynaud[3], R. Röthlisberger[16], U. Ruth[10], O. Rybak[10], M. Severi[4], J. Schmitt[10], J. Schwander[6], U. Siegenthaler[6], M.-L. Siggaard-Andersen[7], R. Spahni[6], J. P. Steffensen[7], B. Stenni[22], T. F. Stocker[6], J.-L. Tison[23], R. Traversi[4], R. Udisti[4], F. Valero-Delgado[10], M. R. van den Broeke[20], R. S. W. van de Wal[20], D. Wagenbach[24], A. Wegner[10], K. Weiler[6], F. Wilhelms[10], J.-G. Winther[18] & E. Wolff[16]

[1]Department of Environmental Sciences, University Ca' Foscari of Venice, [2]Institute for the Dynamics of Environmental Processes-CNR, Dorsoduro 2137, 30123 Venice, Italy. [3]Laboratoire de Glaciologie et Géophysique de l'Environnement (LGGE), CNRS-UJF, BP96 38402 Saint-Martin-d'Hères cedex, France. [4]Department of Chemistry, University of Florence, Via della Lastruccia 3, 50019 Sesto Fiorentino, Florence, Italy. [5]EAWAG, PO Box 611, 8600 Dübendorf, Switzerland. [6]Climate and Environmental Physics, Physics Institute, University of Bern, Sidlerstrasse 5, 3012 Bern, Switzerland. [7]Niels Bohr Institute, University of Copenhagen, Juliane Maries Vej 30, 2100 Copenhagen OE, Denmark. [8]Laboratoire des Sciences du Climat et de l'Environnement (LSCE/IPSL), CEA-CNRS-UVSQ, CE Saclay 91191, Gif sur Yvette, France. [9]Environmental Sciences Department, University of Milano Bicocca, Piazza della Scienza 1, 20126 Milano, Italy. [10]Alfred-Wegener-Institute for Polar and Marine Research, Columbusstrasse, D-27568 Bremerhaven, Germany. [11]Max Planck Institute for Mathematics in the Sciences, Inselstrasse 22, 04103 Leipzig, Germany. [12]Alfred Wegener Institute for Polar and Marine Research, Research Unit Potsdam, Telegrafenberg A 43, 14473 Potsdam, Germany. [13]GSF National Center for Environment and Health, Ingolstädter Landstrasse 1, 85764 Neuherberg, Germany. [14]University College London, Gower Street, London WC1E 6BT, UK. [15]Department of Physical Geography and Quaternary Geology, Stockholm University, 106 91 Stockholm, Sweden. [16]British Antarctic Survey, High Cross, Madingley Road, Cambridge CB3 0ET, UK. [17]Departement Geografie, Vrije Universiteit Brussel, Pleinlaan 2, 1050 Brussel, Belgium. [18]Norwegian Polar Institute, 9296 Tromsø, Norway. [19]ENEA, C. R. Casaccia, Via Anguillarese 301, 00060 Roma, Italy. [20]Utrecht University, Institute for Marine and Atmospheric Research, PO Box 80005, 3508 TA Utrecht, The Netherlands. [21]CSNSM/IN2P3/CNRS, Bat. 108, 91405 Orsay, France. [22]Department of Geological, Environmental and Marine Sciences, University of Trieste, Via E. Weiss 2, 34127 Trieste, Italy. [23]Département des Sciences de la Terre, Université Libre de Bruxelles, CP160/03, 1050 Brussels, Belgium. [24]Institute for Environmental Physics, University of Heidelberg, INF229, 69120 Heidelberg, Germany.

Supplemental Material

Age scale:

For the dating of the EDML and EDC ice cores (Figure S1) we used for the first time a new common time scale developed for Greenland and Antarctic ice core records. Central to this EDC3 time scale is a glaciological flow model[1] for the Dome C ice core, where ice flow is relatively simple due to its dome position. Accumulation rate changes in the core are estimated from the dependence of the saturation water vapor pressure on temperature[2] which itself is reconstructed from δD Free parameters (current accumulation rate, the temperature sensitivity controlling the glacial-interglacial accumulation amplitude as well as the sliding ratio, a vertical deformation parameter and the basal melting rate controlling the flow) are constrained in the model by various tie windows around absolute time markers. For the time period of the last 150.000 years discussed here those times are defined by volcanic horizons, rapid methane variations during glacial/interglacial transitions, or ^{10}Be anomalies which have been absolutely dated using the annual layer counted Greenland Ice Core Chronology (GICC05)[3-5] or have also been found in other radiometrically dated archives. The absolute dating uncertainty of this new EDC3 age scale is 1000 years for an age of 41,000 years and better than 2000 years for termination II with the error increasing for older ages. For internal coherence, a corresponding age scale (EDML1) has been derived for EDML by synchronizing the EDML and EDC ice cores using volcanic and dust tie points based on continuous sulfate, electrolytic conductivity, dielectric profiling, particulate dust and Ca^{2+} data available for both cores. Due to the common change in the Patagonian dust source strength and the hemispheric significance of major volcanic eruptions this procedure is justified. The multitude of unambiguous volcanic markers allowed for a synchronization to within typically 20 years or better for the last 75,000 years, which are the main focus of this paper. Between widely separated tie-points the maximum uncertainty occasionally can increase up to 140 years. The synchronization is better than 1000 years at the beginning of MIS5.5 and increasingly

deteriorates for older ages in MIS6, where the synchronization relies on less unambiguous dust concentration changes. Beyond that a dust synchronization has not been achieved. Therefore, we restrict the discussion of our records to the last 150,000 years, where crossdating of the EDML and EDC core is sufficiently constrained.

In order to study the phase relationship between Greenland and Antarctica during MIS2-3 in more detail the EDML and NGRIP ice cores have been synchronized for the time span of the last 55 kyr using the global signal in atmospheric CH_4. This provides an age scale which may still be affected by systematic dating errors; however for this paper the important issue is that it synchronizes the two cores with an uncertainty that is governed mainly by the uncertainty in the ice age-gas age difference at the EDML site. The synchronization is based on a composite high resolution CH_4 record for Greenland. The highest resolution record is from NGRIP. Unfortunately this record covers so far only the period 48 to 38 kyr BP [6]. After 38 kyr BP we used GRIP data and before 48 kyr BP GRIP and GISP data [7]. GRIP and GISP CH_4 data were assigned a NGRIP gas age as follows: For each GRIP CH_4 value we find the depth where the age of the ice is the same as the age of the CH_4 value using the original GRIP Δage calculation [8]. Applying the match points from Rasmussen et al.[9] we find the corresponding depth in the NGRIP ice core. With the NGRIP time scale we calculate a new age which is also the new gas age of the GRIP CH_4 data point on the NGRIP time scale. Note that no new Δage calculation is applied. GISP values were used only before 48 kyr BP. The GISP data was matched on the NGRIP data before 55 kyr BP [10] and after 48 kyr BP. GISP CH_4 data in the gap of the NGRIP data was assigned a NGRIP age by interpolation.

Three similar synchronization methods have been used to assess the temporal coupling of both hemispheres. In the first method the high resolution Greenland composite CH_4 record has been matched with the EDML CH_4 record, making use of the global signal in atmospheric

CH_4 changes. For NGRIP we use the Δage confirmed by the synchronous effect of a fast temperature change in the ice and the gas record[10]. For EDML Δage was estimated using a firnification model[8]. Using the NGRIP age scale and the Δage at both sites we arrive at a synchronized time scale for the Greenland and Antarctic $\delta^{18}O$ records. The result of this approach has been displayed in Figure 3 of the main text. Figure S2 shows the magnitude of Δage for DML, GRIP (after 38kyr BP) and NGRIP (before 38Kyr BP). Δage for NGRIP is larger than for GRIP mainly due to the lower accumulation rate at NGRIP relative to GRIP. The shaded areas show an estimate for the uncertainty of the Δage calculation assuming 25% higher or lower accumulation rates. The effect on Δage is about equivalent to a 10% change in temperature. We estimate the total synchronization uncertainty at the start of DO events adding in quadrature the uncertainties for the synchronization of the CH_4 records and the two Δages for DML and the Greenland composite. Based on the resolution and the structure of the CH_4 records we estimate that the uncertainty for the CH_4 synchronization is small over the Younger Dryas (about 100 years) and on the order of 200 years for most DO events. For DO events 2 and 3 the uncertainty is larger about 300 years. The total synchronization uncertainty adds to 250 yr for the YD, 500 yr for DO2 and DO3, and about 400 yr for other DO events. In between the rapid CH_4 changes the synchronization uncertainty may be much larger. We estimate about 800 years where little CH_4 variations are found.

In a second approach the EDML CH_4 record, reflecting the temperature changes in the north, has been directly synchronized to the Greenland $\delta^{18}O$ record avoiding the calculation of Δage for the Greenland record but assuming that rapid temperature variations in the north and CH_4 changes occurred simultaneously. In the third approach the high resolution EDML CH_4 record, which is essentially reflecting the temperature changes in the north, has been directly compared to the EDML $\delta^{18}O$ record, representative for temperature changes in the Atlantic

sector of the Southern Ocean. Δage has been estimated in this case using an alternative firnification model[11]. Conclusions on north-south temperature phase relationships in this method are somewhat compromised by the reduced resolution of the CH_4 record in Antarctica but this method avoids again the calculation of Δage for the Greenland records. Method 2 and 3 are not applicable for all temporal changes in the CH_4 record due to the different nature of the CH_4 and $\delta^{18}O$ signal. Nevertheless, all three approaches gave essentially the same results in terms of phasing between Greenland and Antarctic temperature variations. While the three methods differ in their way of synchronization they all share the estimate for the uncertainty in Δage at EDML as the main limiting factor for the accuracy of the synchronization.

The synchronization uncertainty as shown in Figure S2 is only slightly higher than for the Byrd GISP synchronization[7] but a factor 2-3 lower than at low accumulation sites such as EDC and Vostok[12]. An independent check of our CH_4 synchronization of the $\delta^{18}O$ records comes from the ^{10}Be peak at approximately 41,000 years before present. Here the direct synchronization of $\delta^{18}O$ records using ^{10}Be (which is accurate to within ±200 years[13]) and the CH_4 synchronization involving the gas age/ice age difference agree within the synchronization uncertainties. Moving away from the ^{10}Be tie point at 41,000 yr BP the modeled age scale and the CH_4 synchronized age scale deviate by as much as 600 years. Potential reasons for this difference may be systematic errors in the flow model or an error in the gas age/ice age difference or a combination of the two. Given the good correspondence of both synchronizations at 41,000 yr BP, a large systematic error in the gas/ice age difference, however, is unlikely to account for major parts of this offset. In summary the CH_4 synchronization allows a clear one-to-one assignment of AIMs and DO events in Greenland, but restricts the quantification of the exact phase relationship between peak warmth in Antarctica and stadial/interstadial transitions in Greenland to generally better than 400 years.

$\delta^{18}O$ and isotope temperature records

Calculation of the temperature reconstruction at EDC has been previously described[2]. For EDML a similar approach to convert $\delta^{18}O$ to temperature was taken. Surface temperatures T_S (in K) can be derived from the $\delta^{18}O$ records using the current linear gradient (r^2=0.89) of average $\delta^{18}O$ and surface temperature in Dronning Maud Land of 0.82 ‰/°C determined in extensive firn core and snow pit studies[14, 15].

In the case of EDML additional corrections had to be applied to the measured $\delta^{18}O$ data as shown in Figure S3 and described below.

a) sea water correction

Modern $\delta^{18}O$ and δD values in the EDML and EDC ice core reflect the depletion relative to present mean standard ocean water (SMOW). However, during the glacial the water isotopic signature of the ocean $\delta^{18}O_{sw}$ was higher due to the large isotopically depleted land ice masses. Accordingly, this offset of the isotopic signature of the water vapour at its ocean source has to be corrected[16]. We used the ice volume induced $\delta^{18}O$ change in sea water[17] based on a stack of benthic $\delta^{18}O$ sediment records[18] to correct for this effect. For the LGM the $\delta^{18}O$ sea water correction of about 1 ‰ implies an increase of the cooling at EDML relative to the Holocene by about 1.2 °C. The time scale of the sea water $\delta^{18}O$ record[17] was matched with EDC3/EDML1 by synchronizing high latitude temperatures[17] with the EDC δD record. Any age scale errors in the sea level corrected $\delta^{18}O$ data are thereby minimised, however, such errors are small on millennial time scales because sea level changes are slow.

b) altitude/upstream correction

In contrast to the EDC ice core, which is located on a dome position, the EDML ice core lies on a gently sloping ridge near a saddle point with small but non negligible (about 1m/yr) horizontal flow velocities for most of the upstream flank. Accordingly, deeper ice at EDML originates from upstream positions at higher altitudes while the ice at Dome C essentially originates at the current drill site over the entire length of the core. Using a nested 3

dimensional flow model[19, 20] we can e.g. show that ice at an age of 150,000 years in the EDML ice core was deposited approximately 160 km upstream, i.e. about 240 m higher in altitude. In addition, overall altitude changes of the ice sheet during past climate conditions also affect the local $\delta^{18}O$ signal at the site of deposition. In essence, measured $\delta^{18}O$ values deeper in the core are representative for the site of upstream deposition and not the current drill site. Accordingly, a systematic decline in $\delta^{18}O$ due to the higher altitude and lower temperature is expected. Using the 3D flow model nested into a large scale ice sheet model we were able to reconstruct both the upstream site of deposition as well as the overall altitude change of the ice sheet at that site. The latter elevation changes are primarily driven by local accumulation changes.

Subsequently we used the recent linear gradient (r^2=0.90) between $\delta^{18}O$ and altitude of -0.96 ‰ /100 m derived from the snow pit and shallow firn core data[14, 15] to correct the measured and sea level corrected $\delta^{18}O$ signal to our drill site location. For instance in MIS5.5, this leads to a correction in $\delta^{18}O$ of about +2.7 ‰, translating to a warming of 3.3 °C. Sea water and upstream/altitude corrected as well as uncorrected $\delta^{18}O$ and δD values are shown in Figure S3 together with sea level changes and upstream altitudes of snow deposition. The error introduced by these corrections is mainly determined by the accuracy of the modeled overall elevation changes which can be estimated to be ± 50 m which translates into a $\delta^{18}O$ error of ± 0.5 ‰ equivalent or a surface temperature error of ± 0.6 °C.

c) accumulation rates

Accumulation rates e.g. used in the CH_4 synchronization were estimated from the thermodynamic dependence of precipitation rate on the temperature at the elevation of cloud formation over the ice sheet[2]. This inversion temperature T_I (in °K) at the site and time of deposition is deduced from the sea level (but not upstream) corrected $\delta^{18}O$ record assuming a linear relationship between surface and inversion temperature at EDML as shown for the East Antarctic plateau[21], i.e.

$T_I = 0.67 T_s + 88.94$

The local accumulation rate is then calculated (similar as for EDC[2]) according to

$$A=A_0*f(T_I)/f(T_I^0)*(1+\beta(T_I-T_I^0))$$

where T_I^0 is the present-day inversion temperature at the EDML drill site (242.20 K) assuming that the very good linear spatial relationship between altitude and temperature today holds also back in time. A_0 is the present-day accumulation rate of 64 $kgm^{-2}yr^{-1}$ at the EDML drill site, β is a constant fitting parameter, and $f(T_I)$ is given by:

$$f(T_I)=(B_s/T_I-1)/T_I^2 * \exp(-B_s/T_I)$$

where B_s=6148.3 K and an equivalent relation holds for $f(T_I^0)$. The f function basically takes into account the temperature dependent change of saturation vapour pressure, whereas the parameter β takes into account glacial-interglacial changes of accumulation that are not explained by this relationship. β=0.045 has been empirically determined by fitting the spatial variation in recent upstream accumulation rates derived from firn cores[14, 15] and an extended surface radar survey[22, 23]. This leads to average glacial accumulation rates around the EDML drill site which are around 45 % of current values. For the glacial period the error introduced by the altitude correction is less than 15 %. However for the glacial period potential changes in water vapour transport may come into play which may affect the application of the recent spatial $\delta^{18}O$/temperature gradient. Modelling results[16] show that this effect is much smaller than for the Greenland ice sheet. Accordingly, we estimate the glacial accumulation rates to be accurate within ± 30 %. For MIS5.5 the average reconstructed accumulation at the drill site is 102 $kgm^{-2}yr^{-1}$. The MIS5.5 accumulation rate at the place of deposition, on the other hand, is found to be similar to today's value at EDML. That is because despite in general warmer climatic conditions during MIS5.5 the ice originated from a location with colder and drier conditions than in the EDML drill site region. Because circulation is expected to be similar for MIS5.5 and Holocene conditions the main error for the accumulation rate estimate during MIS5.5 stems from the altitude correction, which amounts to about ± 0.7 cm water equivalent / year or less than 10%.

References

1. Parrenin, F., Jouzel, J., Waelbroeck, C., Ritz, C. & Barnola, J.-M. Dating the Vostok ice core by an inverse method. Journal of Geophysical Research 106, 31837-31851 (2001).
2. EPICA community members. Eight glacial cycles from an Antarctic ice core. Nature 429, 623-628 (2004).
3. Rasmussen, S. O. et al. A new Greenland ice core chronology for the last glacial termination. Journal of Geophysical Research 111, D06102 (2006).
4. Andersen, K. K. et al. The Greenland Ice Core Chronology 2005, 15-42 kyr. Part 1: Constructing the time scale. Quaternary Science Reviews, accepted (2006).
5. Svensson, A. et al. The Greenland Ice Core Chronology 2005, 15-42 kyr. Part 2: Comparison to other records. Quaternary Science Reviews, accepted (2006).
6. Flückiger, J. et al. N_2O and CH_4 variations during the last glacial epoch: Insight into global processes. Global Biogeochemical Cycles 18, GB1020 (2004).
7. Blunier, T. & Brook, E. J. Timing of millennial-scale climate change in Antarctica and Greenland during the last glacial period. Science 291, 109-112 (2001).
8. Schwander, J. et al. The age of the air in the firn and the ice at Summit, Greenland. Journal of Geophysical Research 98, 2831-2838 (1993).
9. Rasmussen, R. A. et al. Synchronisation of the NGRIP, GRIP, and GISP2 ice cores across MIS2 and palaeoclimatic implications. Quaternary Science Reviews, submitted (2006).
10. Huber, C. et al. Isotope calibrated Greenland temperature record over Marine Isotope Stage 3 and its relation to CH_4. Earth and Planetary Science Letters 245, 504-519 (2006).
11. Goujon, C., Barnola, J. M. & Ritz, C. Modeling the densification of polar firn including heat diffusion: application to close-off characteristic and gas isotopic

fractionation for Antarctic and Greenland sites. Journal of Geophysical Research 108, 4792 (2003).

12. Blunier, T. et al. Asynchrony of Antarctic and Greenland climate change during the last glacial period. Nature 394, 739-743 (1998).

13. Raisbeck, G., Yiou, F. & Jouzel, J. Cosmogenic ^{10}Be as a high resolution correlation tool for climate records. Geochimica et Cosmochimica Acta 66, A623 (2002).

14. Oerter, H. et al. Accumulation rates in Dronning Maud Land, Antarctica, as revealed by dielectric-profiling measurements of shallow firn cores. Annals of Glaciology 30, 27-34 (2000).

15. Graf, W. et al. Stable isotope records from Dronning Maud Land, Antarctica. Annals of Glaciology 35, 195-201 (2002).

16. Jouzel, J. et al. Magnitude of isotope/temperature scaling for interpretation of central Antarctic ice cores. Journal of Geophysical Research 108, 4361 (2003).

17. Bintanja, R., van de Wal, R. S. W. & Oerlemans, J. Modelled atmospheric temperatures and global sea levels over the past million years. Nature 437, 125-128 (2005).

18. Lisiecki, L. E. & Raymo, M. E. A Pliocene-Pleistocene stack of 57 globally distributed benthic δ^{18}O records. Paleoceanography 20, PA1003 (2005).

19. Huybrechts, P. Sea-level changes at the LGM from ice-dynamic reconstructions of the Greenland and Antarctic ice sheets during the glacial cycles. Quaternary Science Reviews 21, 203-231 (2002).

20. Pattyn, F. A new three-dimensional higher-order thermomechanical ice sheet model: basic sensitivity, ice stream development, and ice flow across subglacial lakes. Journal of Geophysical Research 108, 2382 (2003).

21. Jouzel, J. & Merlivat, L. Deuterium and oxygen 18 in precipitation: Modeling of the isotopic effects during snow formation. Journal of Geophysical Research 89, 11749-11757 (1984).

22. Rybak, O., Huybrechts, P., Steinhage, D. & Pattyn, F. Dating and accumulation rate reconstruction along the Dome Fuji - Kohnen radio-echo-sounding profile. Geophysical Research Abstracts 7, 05421 (2005).

23. Steinhage, D., Nixdorf, U., Meyer, U. & Miller, H. Subglacial topography and internal structure of central and western Dronning Maud Land, Antarctica, determined from airborne radio echo sounding. Journal of Applied Geophysics 47, 183-189 (2001).

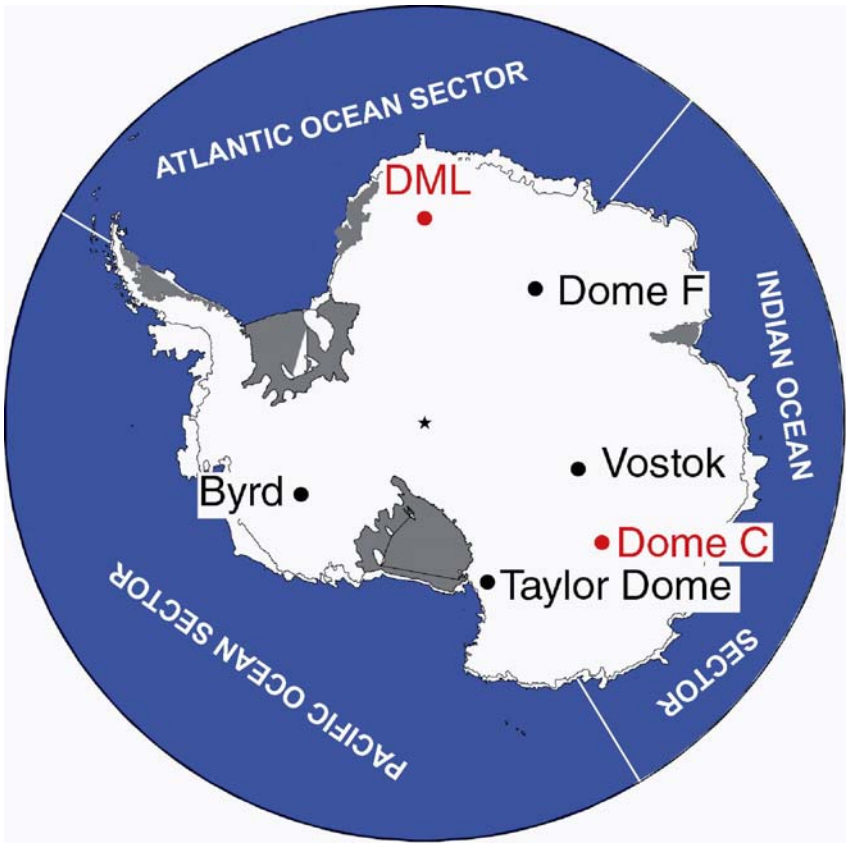

Figure S1: Map of the Antarctic continent indicating the EPICA drill sites in Dronning Maud Land (DML) and at Dome C together with previously drilled deep ice cores.

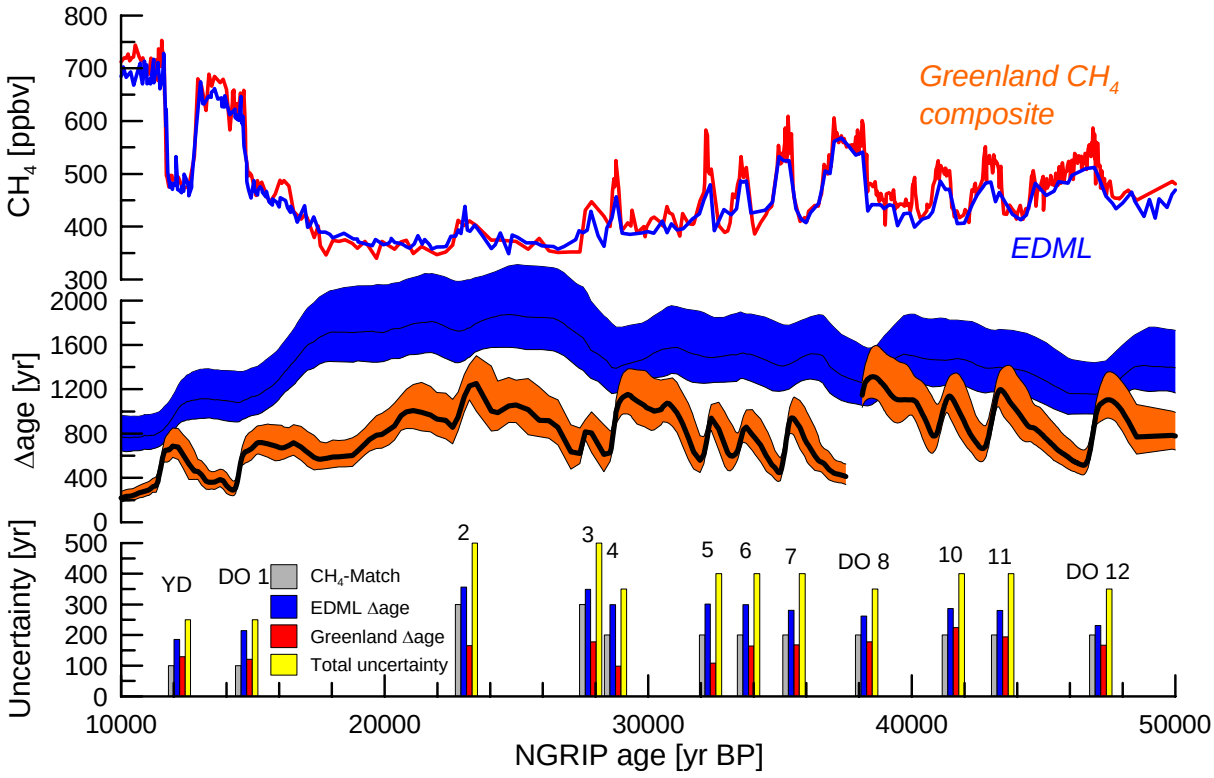

Figure S2: Top: CH_4 records for Greenland and EDML. Middle: Δage with uncertainty corresponding to a 25% change in accumulation. The effect is comparable to a 10% change in temperature. Blue for EDML and red for the Greenland composite, respectively. Before 38 kyr BP the synchronization is based on NGRIP data and the NGRIP Δage is shown. After 38kyr the synchronization is based on GRIP CH_4 data and the GRIP Δage is shown. Bottom: Contributions to the synchronisation uncertainty for individual rapid climate changes. Grey bar represents the uncertainty of the CH_4 synchronization. Blue and Red bars show the uncertainty of Δage assuming a 25% change in accumulation for EDML and the Greenland composite, respectively. The three components are added in quadrature to a total uncertainty for the synchronization of the ice records (yellow bars).

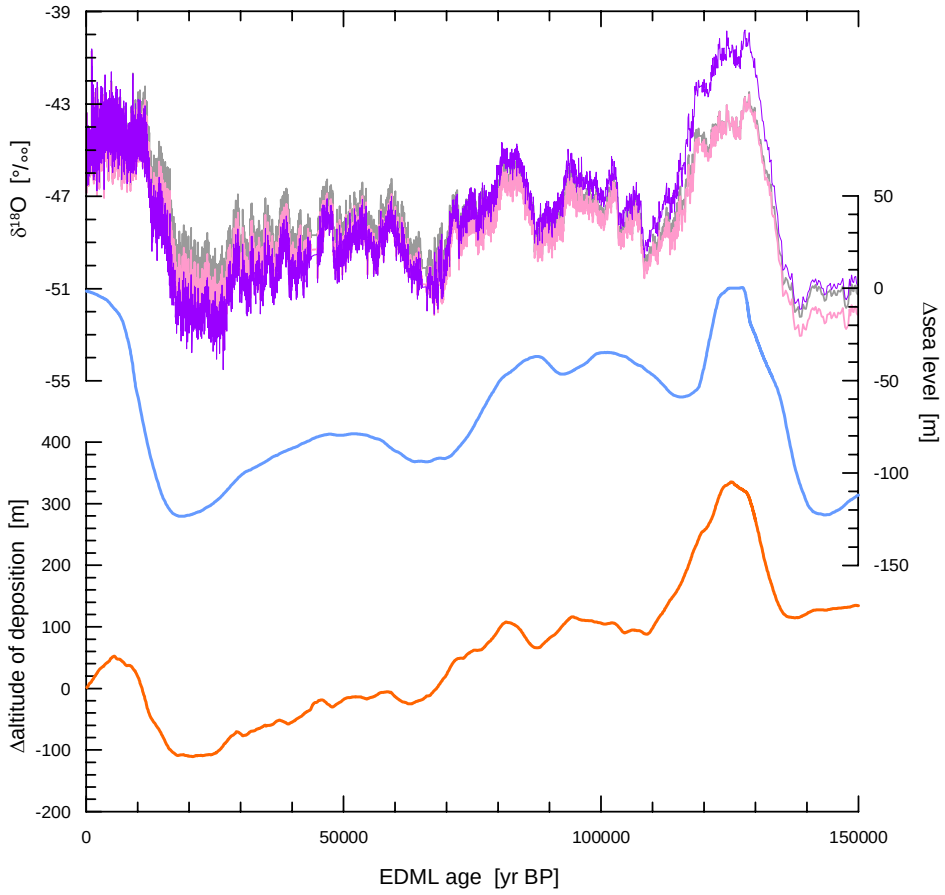

Figure S3: Top: Corrected $\delta^{18}O$ record at EDML: measured $\delta^{18}O$ data representative for the upstream site of deposition (grey); sea level corrected $\delta^{18}O$ data representative for the upstream site of deposition (pink); sea level and upstream corrected $\delta^{18}O$ record representative for the EDML current drill site (purple). Middle: Sea level changes used for the correction as derived from benthic $\delta^{18}O$ and ice sheet modeling[17]. The strongest effect is encountered for peak glacial periods where the continental ice volume was largest; Bottom: Elevation of the initial place of snow deposition relative to the current drill site at 2892m a.s.l. determined by a high-resolution higher order flow model[20] nested in a 3D large ice sheet model[19] used for altitude/upstream correction. This curve comprises both upstream effects (long-term upward trend in the correction) as well as local altitude changes of the ice sheet at the site and time of snow deposition in the past (variations around the long-term trend)[19].

an independent group working on the genetic basis of anxiety has implicated ROS metabolism in this complex trait[6]. Are the behavioural changes in the PGC-1α-deficient mice also due to an absence of antioxidant defences? If so, does this imply that what cell biologists call oxidative stress and what social scientists call psychological stress might ultimately share a common mechanism? Further study is necessary, but people who fear public speaking may take some comfort in the notion that the problem might not be in their head but rather, more specifically, in their mitochondria.

The work of Spiegelman and colleagues[1] brings up another interesting aspect of mitochondrial biology. It is well known that these organelles, whether they come from simple organisms or complex mammals, all leak measurable amounts of ROS. Experimental systems that simply increase the production of antioxidant proteins seem to be quite effective at reducing this leakage. If ROS synthesis is so bad, and a molecular solution so apparently straightforward, why has this 'design flaw' not been eradicated during the billions of years of evolution? There are many possible answers, but one is that the notion that ROS from the mitochondria are solely harmful could be incorrect. Indeed, substantial evidence exists that ROS generated in the cytoplasm could have vital signalling functions[7], and this might also be true for oxidants derived from mitochondria[8,9]. The new study[1] strengthens this possibility and suggests that a homeostatic loop exists between mitochondria and ROS and that this loop is, at least in part, orchestrated by PGC-1α (Fig. 1).

Previous reports have suggested that certain life-extending strategies, such as calorie restriction, might work through the PGC-1α-induced mitochondrial biogenesis programme[10]. Spiegelman and colleagues' study suggests that PGC-1α could also alter our susceptibility to neurodegenerative conditions that are linked to mitochondrial dysfunction and oxidative stress, such as Parkinson's disease. Therefore, fine-tuning the activity of this resourceful coactivator might have a wide range of clinical benefits, including potentially allowing us to live longer and think more clearly. Not a bad set of objectives, especially if we are ultimately going to need to tackle really tricky problems like global warming. ■

Toren Finkel is in the Cardiology Branch, NHLBI, National Institutes of Health, 10/CRC 5-3330, 10 Center Drive, Bethesda, Maryland 20892, USA.
e-mail: finkelt@nih.gov

1. St-Pierre, J. *et al. Cell* **127,** 397–408 (2006).
2. Finck, B. N. & Kelly, D. P. *J. Clin. Invest.* **116,** 615–622 (2006).
3. Puigserver, P. *et al. Cell* **92,** 829–839 (1998).
4. Lin, J. *et al. Cell* **119,** 121–135 (2004).
5. Leone, T. C. *et al. PLoS Biol.* **3,** e101 (2005).
6. Hovatta, I. *et al. Nature* **438,** 662–666 (2005).
7. Finkel, T. *Curr. Opin. Cell Biol.* **15,** 247–254 (2003).
8. Nemoto, S., Takeda, K., Yu, Z. X., Ferrans, V. J. & Finkel, T. *Mol. Cell Biol.* **20,** 7311–7318 (2000).
9. Werner, E. & Werb, Z. *J. Cell Biol.* **158,** 357–368 (2002).
10. Lopez-Lluch, G. *et al. Proc. Natl Acad. Sci. USA* **103,** 1768–1773 (2006).

CLIMATE CHANGE

The south–north connection

Eric J. Steig

A new ice-core record from Antarctica provides the best evidence yet of a link between climate in the northern and southern polar regions that operates through changes in ocean circulation.

Over the past 20 years, the analysis of ice cores has been transforming our understanding of past climate. Most notably, the Vostok core from Antarctica[1] provided remarkable evidence of the correspondence between temperature and atmospheric carbon dioxide concentrations over the past 420,000 years. And the GISP2, GRIP and NGRIP cores from Greenland[2,3] offered a view in unprecedented detail of climate change over the past 100,000 years (including the revelation that abrupt warming events of 10 °C or more have taken place in Greenland).

More recently, the European Project for Ice Coring in Antarctica (EPICA) obtained the longest ice-core record yet[4], one spanning 800,000 years of climate history, from Dome C, in the same sector of Antarctica as Vostok. The EPICA team has now pulled off another feat. As it reports on page 195 of this issue[5], it has completed analysis of 2,500 metres of an ice core from Dronning Maud Land in the Atlantic sector of Antarctica (Fig. 1).

The significance of this 'EDML' core is not its sheer length; at the site concerned, 2,500 m takes us back 150,000 years. Rather, it is its resolution: this is the highest-resolution record obtained outside Greenland that extends well beyond the last glacial maximum (about 20,000 years ago). In consequence, the EPICA team has been able to place the EDML record with high precision on the same timescale as the records from Greenland. This allows us to compare the Greenland and Antarctic records over time intervals as short as a few centuries.

At this point, an analogy may help. On a year-to-year basis, much global climate variability is dominated by the El Niño–Southern Oscillation (ENSO). Understanding ENSO has required comparison of climate records in the main ENSO region (the tropical Pacific) with records elsewhere. This could not have been achieved without placing different time-series data on the same timescale. We would otherwise have little confidence, for example, in the observed correspondence between ENSO and rainfall variations in southern California. Nor would it be meaningful to try to understand the ocean and atmospheric dynamics that give rise to that relationship, because we could not reject the null hypothesis that it was merely due to chance. The Greenland and Antarctic ice-core records are likewise measures of climate variability, but on timescales of centuries, millennia and longer. Indeed, the high-resolution measures of climate afforded by ice-core records show unambiguously that climate varies on these longer timescales much more widely than one would expect from simple extrapolation of the power spectrum of observed (modern) climate[6].

The usual explanation for the millennial-scale variability is that it is due to changes in the deep meridional overturning circulation (MOC) in the Atlantic Ocean. Put simply, a vigorous MOC is thought to deliver heat to the North Atlantic at the expense of the Southern Ocean. Increases and decreases in MOC strength should thus result in a climate 'see-saw' between the Southern and Northern

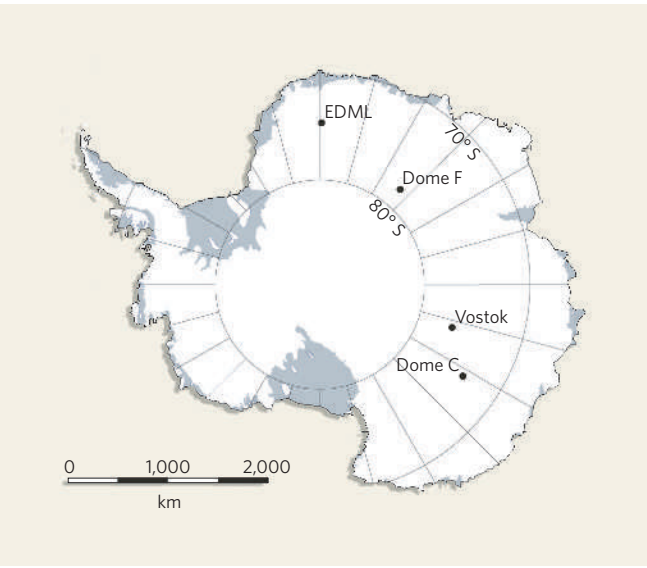

Figure 1 | Core sites. Locations of deep ice-core drilling projects in Antarctica where records longer than 100,000 years have been obtained. The new EDML core[5] in Dronning Maud Land has the highest time resolution of these cores.

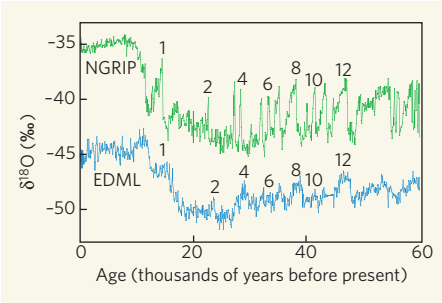

Figure 2 | Core data. Comparison of records from the EDML ice core from Antarctica[5] and the NGRIP core from Greenland[3]; oxygen-isotope ($\delta^{18}O$) ratios are a measure of temperature. Temperatures increase gradually in Antarctica, reaching a maximum at about the same time that Greenland warms rapidly. The numbers refer to designated warming events in Greenland and the corresponding Antarctic temperature maxima. Statistically, the records are largely coherent for time periods down to around 800 years, which is similar to the relative dating uncertainty. Thus, the Greenland and Antarctic climates are meaningfully related on timescales as short as measurement precision allows.

Hemispheres[7]. An observation cited in support of this idea is that there is an out-of-phase relationship between Antarctic and Greenland ice-core records of temperature (or rather, of oxygen and deuterium isotope ratios, which are well-established proxies for temperature)[8]. The problem has been that — unlike in the ENSO analogy — there is considerable uncertainty in the dating. Analyses of the existing records have generally shown that the relationship between the Greenland and Antarctic records is weak and not statistically significant, except on the very longest timescales associated with well-understood astronomical factors (the Milankovich forcing of ice ages)[9]. So it has been difficult to rule out the null hypothesis that the variability in these records largely reflects regional phenomena such as variations in wind patterns or sea-ice extent.

This is where the EDML results come in. They show that the Antarctic and Greenland ice-core records are meaningfully related, and on quite short timescales. In particular, comparison of the oxygen-isotope records shows that one can make a direct link between the distinctive temperature maxima in the Antarctic record (at least going back 60,000 years) and the unambiguous abrupt warmings in Greenland (Fig. 2). Not every Antarctic temperature maximum is as distinct as the Greenland warmings; for example, it is not clear why the small maxima labelled 6 and 10 in Fig. 2 should count as 'events', but the similarly sized bumps between maxima 1 and 2 should not. But the relationship is too strong to be due to chance.

In fact, for the interval 20,000 to 90,000 years ago a remarkable 40% of the variance in the Greenland records can be explained by the EDML time series. A more rigorous estimate of the spectral coherence between the records shows that this significant relationship extends to timescales as short as a few centuries. Furthermore, there is a consistent out-of-phase relationship between the records. They are not strictly 'antiphased', as the term see-saw would imply. Rather, the average phase relationship is about 90°. Although cold conditions in Greenland tend to be associated with warming in Antarctica, and vice versa, the peak warmth in both records actually occurs at about the same time.

Does the EDML record demonstrate the dominant influence of the MOC on climate variability? This is not just an academic question. Variations in this circulation have been invoked to explain everything from the abrupt climate changes observed in the Greenland records to the Little Ice Age (a period of cooling between about AD 1400 and 1900 in the North Atlantic region). And the possibility of a sensitive MOC has been proposed as a 'tipping point' in future human-influenced climate change[10].

One objection to these ideas is that the MOC plays a minor role in the heat budget of the polar regions[11]. Heat transport in the atmosphere is much more important, and the atmosphere might simply compensate for any changes in MOC[12]. Furthermore, the causes of the purported changes in MOC are not understood. The conventional answer — flooding of the North Atlantic Ocean by ice and meltwater from the Laurentide ice sheet in northern North America (so-called Heinrich events) — is not very convincingly supported by the evidence[13].

The EDML data do not directly address these concerns. But they are nonetheless compatible with the idea that the MOC has a central role in millennial-scale variability. What is particularly compelling is that there is a strong linear relationship between the magnitude of warming in Antarctica and the duration of the warm period that follows each abrupt event in Greenland (see Fig. 3 of the paper[5] on page 197). The authors' explanation is simple: the duration of the warm periods in Greenland reflects the duration of reduced MOC, and hence the amount of heat retained in the Southern Ocean. This is consistent with a model[14], proposed a few years ago, in which the magnitude of Antarctic temperature change is controlled by the effective size of the Southern Ocean heat reservoir (including both dynamic and thermodynamic effects). We may have to wait some time before we see whether these results can be reproduced by more sophisticated ocean–atmosphere climate models, because realistically encapsulating the dynamics of the Southern Ocean in such models remains a problem. But we can hope that these new results[5] will inspire the relevant work to be done. ■

Eric J. Steig is in the Department of Earth and Space Sciences, 70 Johnson Hall, University of Washington, Seattle, Washington 98195, USA.
e-mail: steig@ess.washington.edu

1. Barnola, J. M., Raynaud, D., Korotkevich, Y. S. & Lorius, C. *Nature* **329,** 408–414 (1987).
2. Grootes, P. M., Stuiver, M., White, J. W. C., Johnsen, S. & Jouzel, J. *Nature* **366,** 552–554 (1993).
3. North Greenland Ice Core Project members *Nature* **431,** 147–151 (2004).
4. EPICA Community Members *Nature* **429,** 623–628 (2004).
5. EPICA Community Members *Nature* **444,** 195–198 (2006).
6. Huybers, P. & Currey, W. *Nature* **441,** 329–332 (2006).
7. Crowley, T. J. *Paleoceanography* **7,** 489–497 (1992).
8. Blunier, T. *et al. Nature* **394,** 739–743 (1998).
9. Roe, G. H. & Steig, E. J. *J. Clim.* **17,** 1929–1944 (2004).
10. Rahmstorf, S. in *Encyclopedia of Quaternary Sciences* (ed. Elias, S. A.) (Elsevier, Amsterdam, in the press).
11. Seager, R. & Battisti, D. S. in *Global Circulation of the Atmosphere* (eds Schneider, T. & Sobel, A. H.) (Princeton Univ. Press, in the press).
12. Wunsch, C. *Quat. Res.* **65,** 191–203 (2006).
13. Steig, E. *Nature* **439,** 660 (2006).
14. Stocker, T. F. & Johnsen, S. J. *Paleoceanography* **18,** 1087 (2003).

STRUCTURAL BIOLOGY

Enzyme theory holds water

Matthew Freeman

Intramembrane proteases have attracted much attention because of their biological and medical value. The first crystal structure of one of these enzymes begins to solve the mystery of how they work.

Proteases are some of the most potent tools to which a cell has access, because, unlike most other protein-modifying enzymes, they catalyse an essentially irreversible reaction — the breaking of peptide bonds. This can obviously be used to degrade unwanted proteins, but proteases also have many vital regulatory functions[1]. In the past few years, a class of proteases called intramembrane proteases has been discovered. These comprise diverse families, but all have multiple transmembrane domains and an active site apparently embedded within the hydrophobic region of cell membranes.

All intramembrane proteases share the curious property of cutting their membrane-spanning protein targets in the transmembrane regions — that is, they are thought to perform the peptide-cleaving reaction (which requires water) within the lipid bilayer of cellular membranes[2]. As this is an environment where water is traditionally assumed to be in short supply, this is a somewhat heretical idea. This